

SUPPORTING INFORMATION

Seawater-degradable, tough, and fully bio-derived nonwoven polyester fibres reinforced with mechanically defibrated cellulose nanofibres

*Miyu Yamagata,^a Yoshiyasu Nagakawa,^b Mizuki Irie,^c Shin-ichiro Suye,^{a,d} and Satoshi Fujita^{*a,c,d}*

^a Department of Frontier Fiber Technology and Sciences, Graduate School of Engineering, University of Fukui, 3-9-1, Bunkyo, Fukui 910-8507, Japan

^b Biotechnology Group, Tokyo Metropolitan Industrial Technology Research Institute, 2-4-10, Aomi, Koto-ku, Tokyo 135-0064, Japan

^c Department of Materials Science and Biotechnology, Faculty of Engineering, University of Fukui, 3-9-1, Bunkyo, Fukui 910-8507, Japan

^d Life Science Innovation Center, University of Fukui, 3-9-1, Bunkyo, Fukui 910-8507, Japan

***Corresponding author**

Satoshi Fujita

Department of Frontier Fiber Technology and Sciences, Graduate School of Engineering, University of Fukui, 3-9-1, Bunkyo, Fukui 910-8507, Japan

Tel: +81-776-27-9969, Fax: +81-776-27-9969, E-mail: fujitas@u-fukui.ac.jp

Table S1. Compositions of emulsions and electrospun fibres

Sample	Type of CNFs	Concentration of CNF suspension (wt.%)	Composition of CNF/PHBH emulsion	Composition of fabricated fibre or film
S-1.6	Short	1	0.25% CNF/15.0% PHBH	1.6% CNF/98.4% PHBH
S-3.2	(BiNF _i -s, Fma-10005; Sugino Machine)	2	0.50% CNF/15.0% PHBH	3.2% CNF/96.8% PHBH
S-4.8		3	0.75% CNF/15.0% PHBH	4.8% CNF/95.2% PHBH
S-6.3		4	1.00% CNF/15.0% PHBH	6.3% CNF/93.7% PHBH
L-1.6		Long	1	0.25% CNF/15.0% PHBH
L-3.2	(BiNF _i -s, Ima-10005; Sugino Machine)	2	0.50% CNF/15.0% PHBH	3.2% CNF/96.8% PHBH
L-4.8		3	0.75% CNF/15.0% PHBH	4.8% CNF/95.2% PHBH
L-6.3		4	1.00% CNF/15.0% PHBH	6.3% CNF/93.7% PHBH

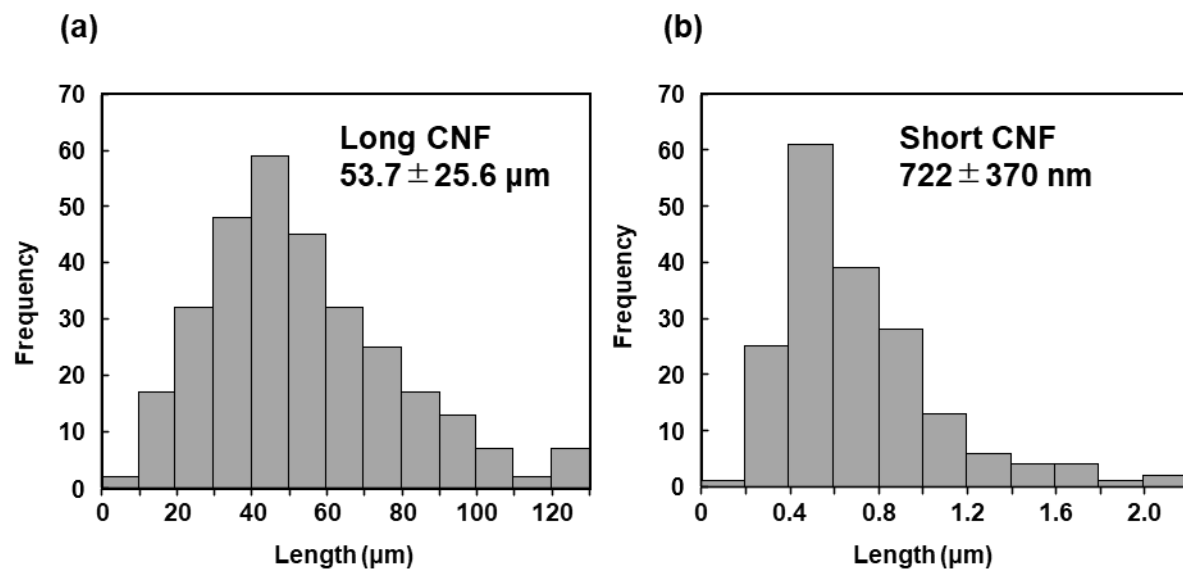


Figure S1. Length distributions of (a) long and (b) short CNFs. CNF samples were dispersed in water and observed by optical microscopy and SEM, respectively. The lengths of fibres were manually measured from the microscopic images by ImageJ.

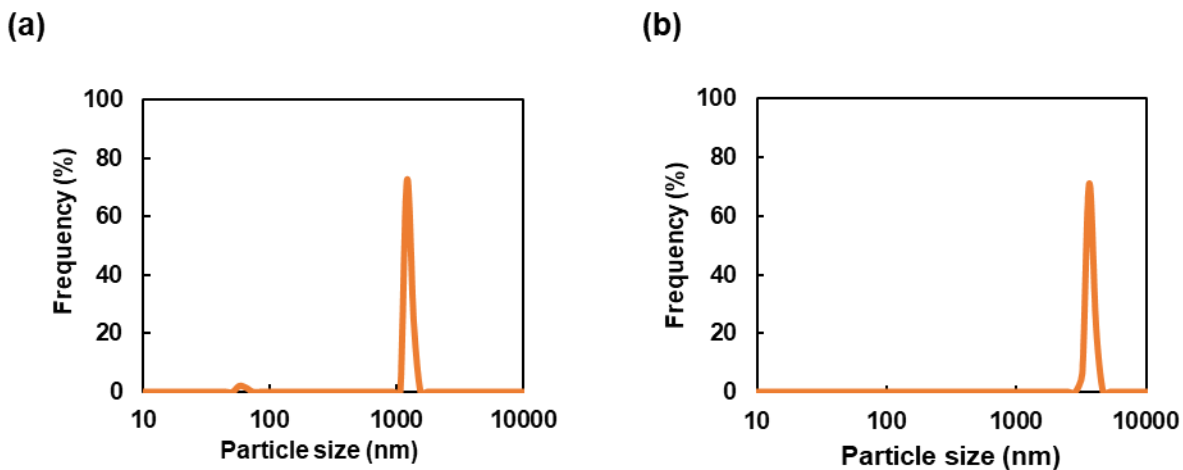


Figure S2. Particle size distributions of (a) L-6.3 and (b) S-6.3 emulsions obtained by DLS.

EXPERIMENTAL

Dynamic light scattering (DLS). To estimate the particle size in the emulsions, 3 mL of each emulsion was placed in a quartz cell and analyzed by DLS (SZ-100, Horiba, Kyoto, Japan) under the following conditions: particle range, 0.1–10,000 nm; wavelength, 532 nm; backscatter angle, 173°; measurement duration, 2 min; and holder temperature, 25 °C.

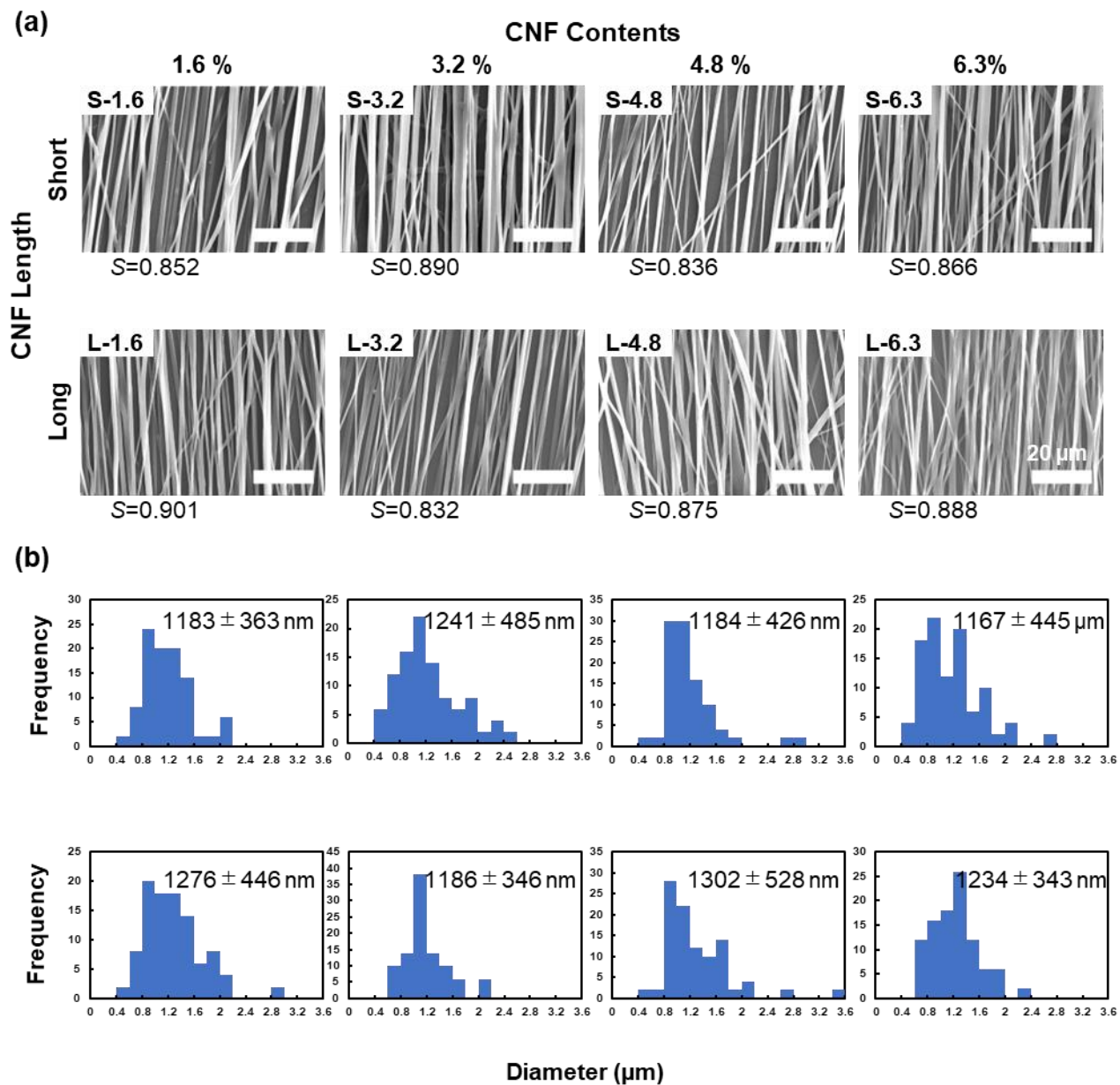


Figure S3. (a) SEM images of aligned electrospun fibres containing CNFs of different lengths and concentrations (scale bar = 20 μm). (b) Distributions of fibre diameters (mean \pm SD).

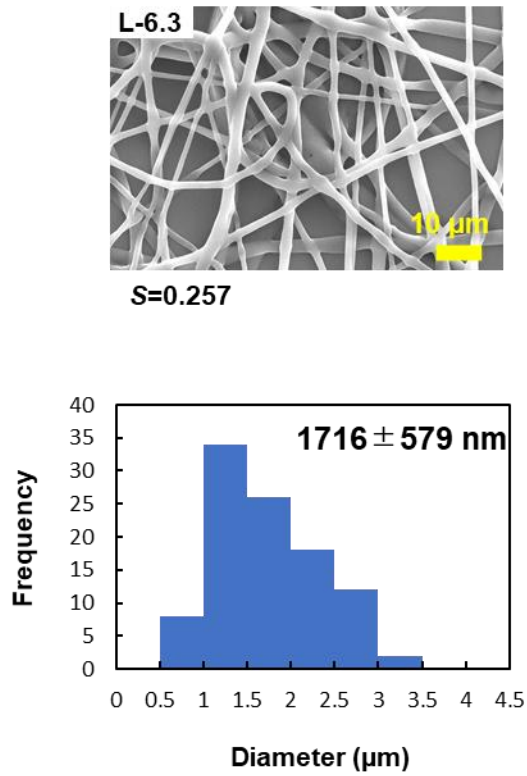


Figure S4. SEM image of randomly oriented L-6.3 fibres and their diameter distribution.

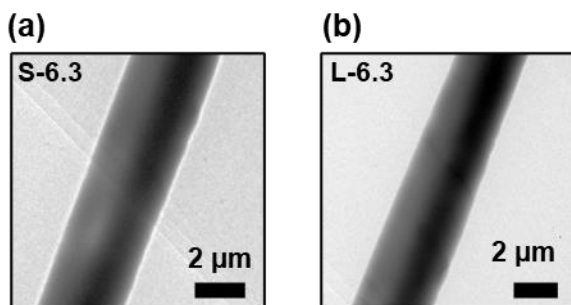
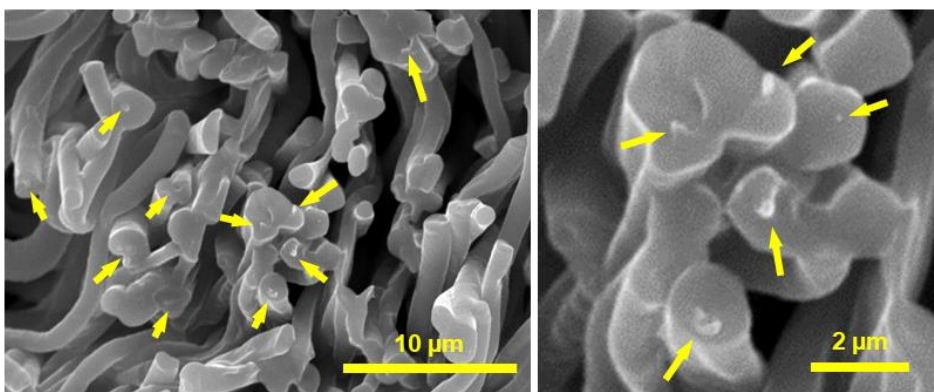
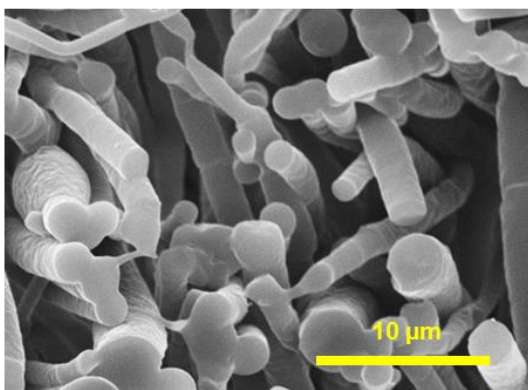


Figure S5. TEM images of single fibres containing (a) short and (b) long CNFs. The electrospinning conditions were identical to those used for acquiring the data in Figure 1e and f.

(a) L-6.3 CNF fibre, Cross section



(b) CNF-free fibre, Cross section



(c) L-6.3 CNF fibre, Cross section

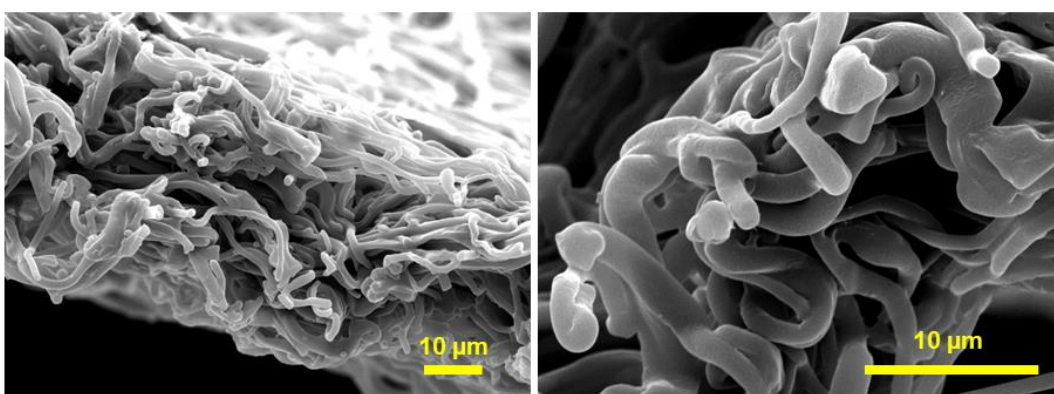


Figure S6. SEM images of cross sections of fibres. (a) L-6.3 CNF-containing fibres. The arrows represent spike-like structures of CNFs. (b) CNF-free fibres. (c) Fracture surface of L-6.3 CNF fibres after the tensile test. No spike-like structures were observed.

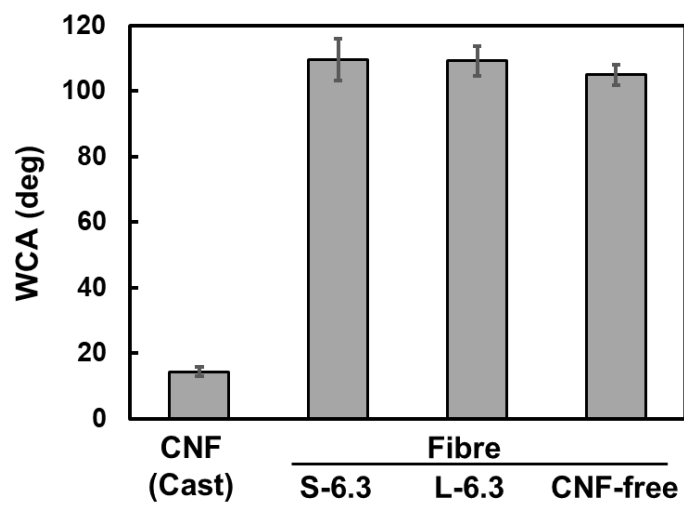


Figure S7. WCAs of CNF cast film and the S-6.3, L-6.3, and CNF-free fibre sheets (n = 3).

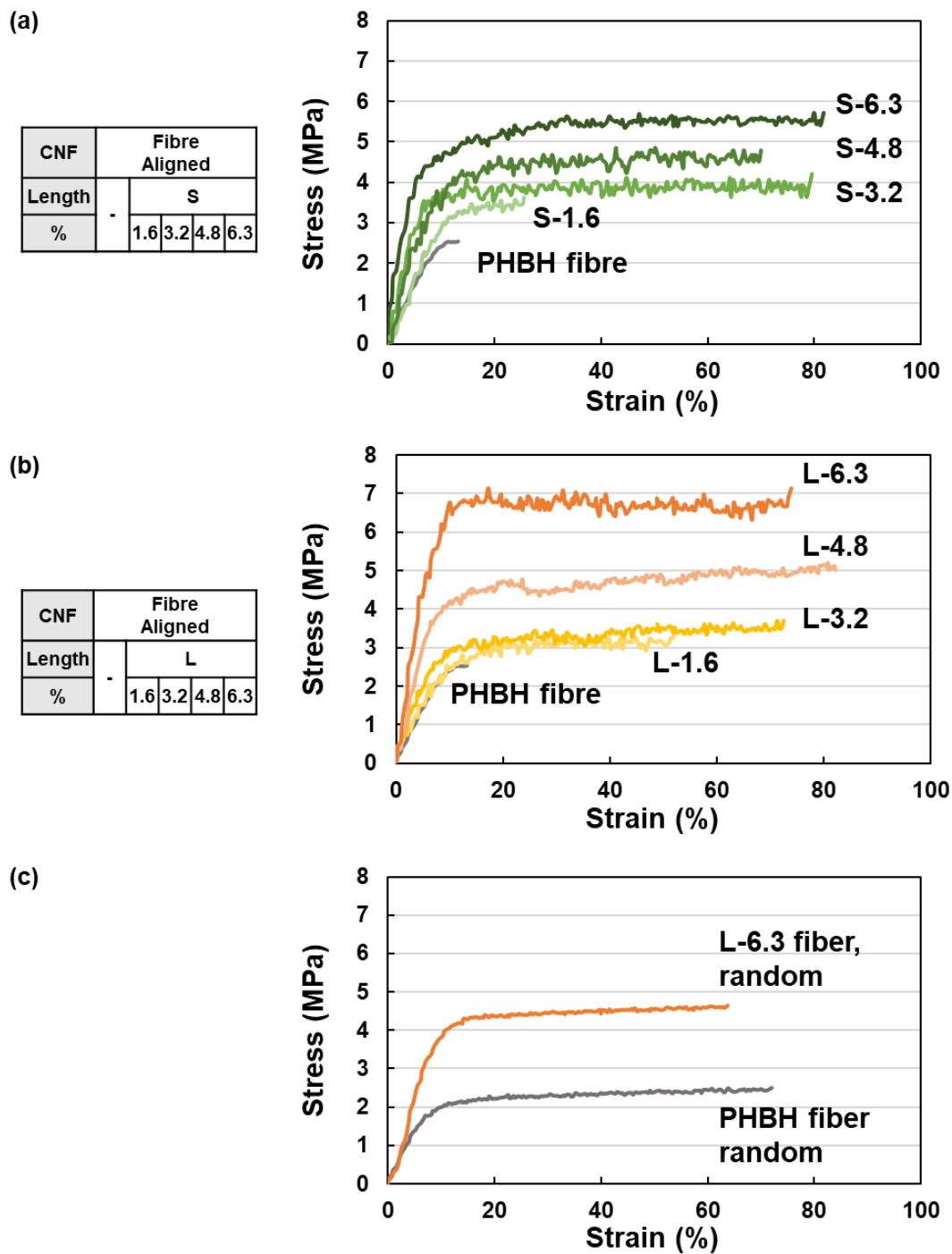


Figure S8. Tensile test results of (a) aligned fibres with short CNFs, (b) aligned fibres with long CNFs, and (c) randomly oriented fibres with/without L-6.3 CNFs.

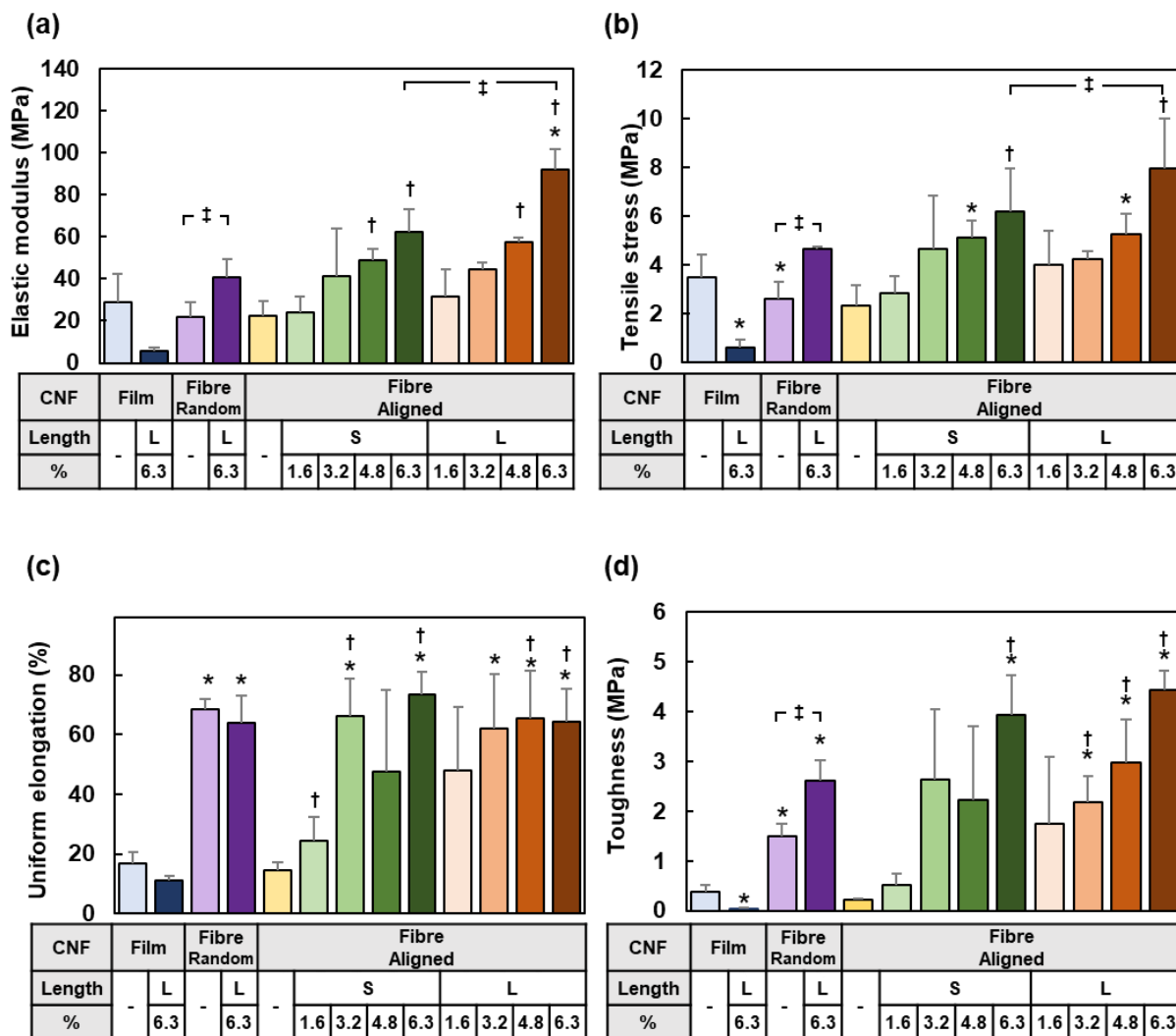


Figure S9. Mechanical properties calculated from the stress–strain curves shown in Figure S8:

(a) elastic modulus, (b) tensile strength, (c) uniform elongation, and (d) toughness.

RESULTS AND DISCUSSION

Tensile tests. Different amounts of CNF with varying lengths were added to the oriented fibres (Figures S8a,b). Both the elastic modulus and tensile strength increased with increasing amounts of short and long CNFs. The elastic modulus, tensile strength, and toughness of the aligned L-6.3

fibres, respectively, were observed to be 1.5, 1.3, and 1.1 times greater than those of the aligned S-6.3 fibres (Figure S9). This difference can be attributed to greater entanglement of CNFs in the fibre cores wherein a large number of long CNFs were localized.

Randomly aligned fibres were also analyzed to investigate the effects of fibre orientation (Figure S8c). Remarkable results in terms of elastic modulus, tensile strength, and toughness were obtained upon addition of CNF to these fibres, indicating that the CNFs also reinforced the core of the randomly oriented fibres. A comparison between the randomly oriented and aligned L-6.3 fibres indicated that the elastic modulus, tensile strength, and toughness of the aligned fibres, respectively, were 2.3, 1.7, and 1.7 times greater than those of the randomly oriented fibres. Similar uniform elongations were achieved in the case of randomly oriented and aligned fibres (Figure S9), which suggests that CNF aggregation in the fibres could be affected by fibre alignment to a certain extent.

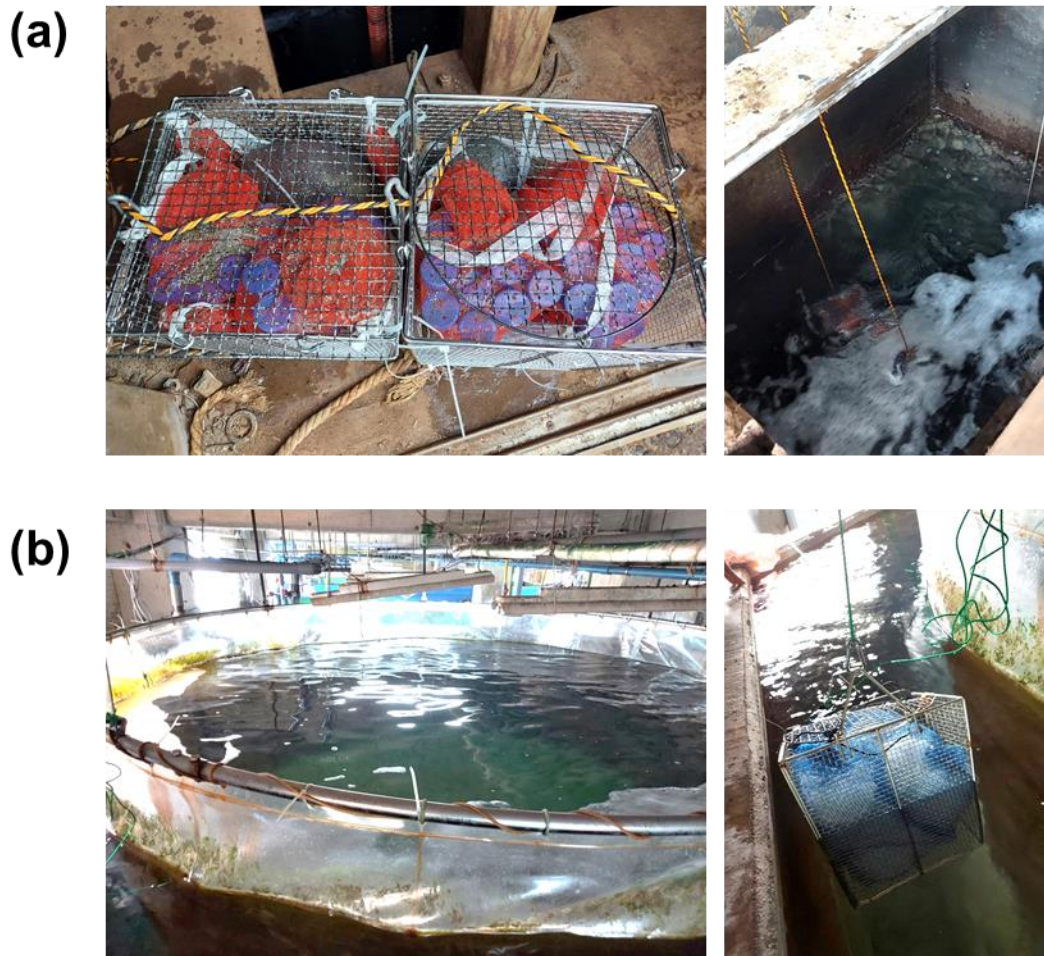


Figure S10. Images of the location where the degradation tests were performed. (a) Samples placed in tubes and immersed in seawater in the pump room, which was influenced by tides and sand. (b) Water tank in which seawater from the pump room was roughly sedimented and statically retained.

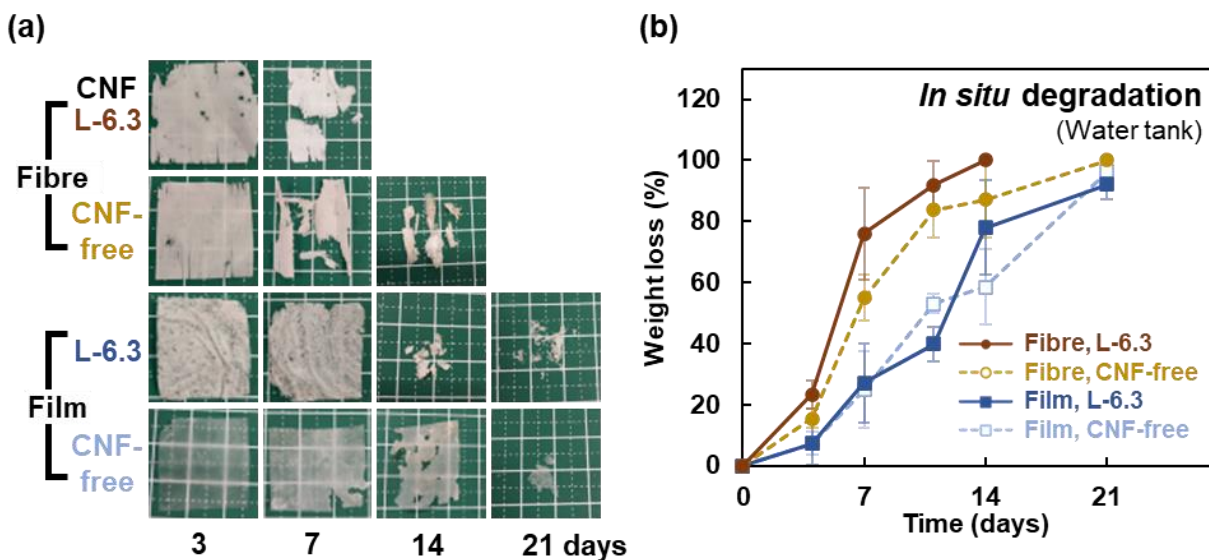


Figure S11. Seawater degradation tests conducted in situ (water tank). (a) Apparent morphologies and (b) weight losses of specimens.

In situ degradation tests in a water tank. Owing to the presence of waves and sand, there was a possibility of physical collapse of the samples during degradation in the pump room. Therefore, additional degradation tests were conducted in a water tank in the backyard of the aquarium (Figure S10b). The water tank was constantly supplied with fresh seawater from the pump room at a constant water current, and the effect of waves and sand was minimal. Thus, the effects of degradation induced by microorganisms were isolated. Fibres immersed in the water tank started showing holes after 3 d and degraded by more than 50% to finally collapse after 7 d. The films showed enhanced surface roughness and degraded completely in 3 weeks (Figure S11).

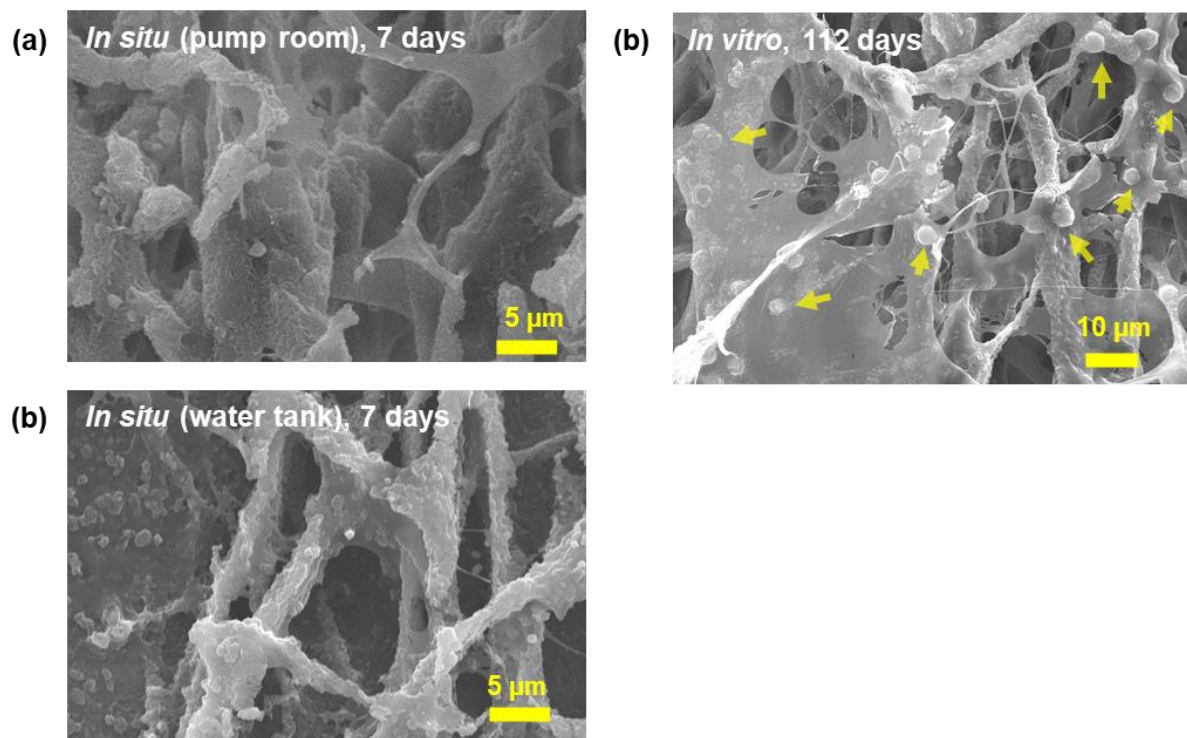


Figure S12. SEM images of degraded aligned L-6.3 fibres after (a) in situ immersion (pump room) for 7 d, (b) in situ immersion (water tank) for 7 d, and (c) in vitro immersion for 112 d. Arrows indicate bacterial adhesion.